Relationship between the Size of the Latex Beads and the Solid−Solid Phase Transitions in Emulsion Polymerized Poly(tetrafluoroethylene)

Carla Marega,* Antonio Marigo, and Valerio Causin

Dipartimento di Scienze Chimiche, Università di Padova, via Marzolo 1, 35131 Padova, Italy

Valerj Kapeliouchko, Emanuele Di Nicolò, and Aldo Sanguineti

Solvay Solexis, Research and Development Center, viale Lombardia 20, 20021 Bollate (MI), Italy

Received April 20, 2004; Revised Manuscript Received May 19, 2004

ABSTRACT: Ten virgin powder samples of poly(tetrafluoroethylene) (PTFE) were examined by differential scanning calorimetry (DSC) and wide-angle X-ray scattering (WAXS). The samples, prepared by emulsion or nanoemulsion polymerization, differed by average molecular weight and particle size. DSC was used to study the trends of the temperature and enthalpy of solid−solid transitions around room temperature. The samples with smaller particle size and lower molecular weight departed heavily from the behavior reported in the literature. The major role of particle size in determining this behavior was established by experiments of crystallization from the melt. WAXS was employed to study the crystalline phases of PTFE as a function of temperature and to confirm the hypotheses put forward in the DSC analysis. WAXS data showed that the degree of order of the crystallites in the virgin powders is controlled by particle size. Therefore, the confinement of the as-polymerized PTFE crystals in small entities (tens of nanometers) has a similar effect on the crystal correlation length and on the solid-state transitions, while it appears that the molecular weight per se is not able to induce such a behavior in the melt-crystallized polymers.

Introduction

Poly(tetrafluoroethylene) (PTFE) has a unique position in the plastics industry due to its inertness, heat resistance, excellent electrical insulation properties, and low coefficient of friction in a wide temperature range. It has a high crystalline melting point (327 °C), very high melt viscosity (10−100 GPa·s at 380 °C), and a high maximum use temperature (>260 °C). In addition, it exhibits unusual toughness down to very low temperatures (<−200 °C); its molecular mass is extremely high (10^6−10^7). It is insoluble in all known solvents and resists attack by most chemicals. Because of its high molecular weight, PTFE does not flow and cannot be easily fabricated by conventional techniques. Therefore, an extensive processing technology had to be developed. The suspension-polymerized PTFE polymer (granular PTFE) is usually fabricated by modified powder metallurgy techniques, and emulsion-polymerized PTFE powders are processed by a cold extrusion process.

Commercial PTFE is manufactured by two different polymerization techniques that result in two different types of chemically identical polymer. Suspension polymerization produces a granular resin, and the polymer particles have a size of some millimeters that can be reduced to a few microns.[1] Emulsion polymerization produces the coagulated dispersion that is often referred to as a fine powder or PTFE dispersion; the average particle size is about 150−300 nm. With conventional polymerization technology, particles with a lower size, down to 100 nm, are obtained only with low conversion reactions.[2] Latexes with particles from 10 to 100 nm are obtained with different technology of polymerization[3,4] on an industrial scale.

* Corresponding author: phone +39-049-8275233; Fax +39-049-8275161; e-mail carla.marega@.unipd.it.

Standard virgin emulsion PTFE particles are made of several ribbons folded together.[5−7] Each ribbon is a highly crystalline extended chain crystallite, whose structure has been attributed to the completely forbidden rearrangement of the polymer chain during the polymerization.[8] The polymer chain axis is believed to be parallel to the longitudinal axis of the ribbon. The folding of the ribbon is dominated by the very high PTFE/water interfacial energy and can be regulated upon changing the polymerization condition. However, the effect of the molecular weight is also important, and extended crystals have been reported to form only at high molecular weight.[9,10]

The most outstanding structural features of PTFE have been described in many papers;[11−18] in particular, the influence of temperature and pressure on polymorphism phenomena in this polymer was studied. The following crystalline phases, investigated at atmospheric pressure, are reported for PTFE: phase IV, hexagonal, showing a 15/7 helix and being stable in the range from 19 to 30 °C; phase II, triclinic, showing a 13/6 helix and being stable below 19 °C; phase I, pseudohexagonal, showing a 15/7 helix at temperatures higher than 30 °C. Finally, phase III, which is only detected at high pressures, has been described to be orthorhombic[17,18] and to have planar zigzag conformation. The temperatures at which transitions from one to another phase occur are referred to as solid−solid transition temperatures.

The aim of this work was to investigate the effect of the particle size (30−260 nm) on the crystal structure, crystal phase transitions, and crystallite dimension. This variable is particularly interesting because microemulsion polymerization allows one to easily obtain particles having sizes comparable to and lower than the crystallite size in PTFE.[19] However, the polymerization conditions did not allow for a complete separation of the

10.1021/ma049238o CCC: $27.50
Published on Web 07/02/2004

Table 1. Particle Radius, Melt Viscosity (η), and Average Molecular Weight ($\bar{M}$) of the Samples

sample	R (nm)	η (Pa·s)	$\bar{M}$ (10^6 g/mol)
L1	15	8.4×10^2	0.13
L2	25	8.3×10^2	0.13
L3	51	4.1×10^2	0.10
L4	96	6.1×10^2	0.11
H1	17	2.3×10^4	0.3
H2	32	6.2×10^6	1.8
H3	34	8.7×10^6	2.0
H4	47	4.7×10^7	3.4
H5	118	2.6×10^{11}	44
H6	131	5.0×10^{11}	54

particle size from the molecular weight, and therefore its effect is also discussed. For the sake of comparison, the same samples after melt crystallization have also been studied.

The analysis was carried out by differential scanning calorimetry (DSC) and wide-angle X-ray scattering (WAXS).

Experimental Section

Samples Preparation. The samples characterized in this work were produced using two different polymerization routes. Samples H5 and H6 are standard commercial emulsion polymerized PTFEs,[1] while all the other samples were polymerized using Solvay Solexis proprietary microemulsion technology.[20] In this technology microemulsion droplets act as nucleation sites in the initial stage of the polymerization.[21] The microemulsions used in this work were prepared with perfluoropolyether oils and surfactants which are commercially available from Solvay Solexis under the trade name Galden and Fomblin. Both polymerization procedures lead to stable colloidal dispersions with a solid content ranging from 15 to 30%. The virgin powders used in this work were obtained by coagulation with nitric acid followed by thorough washing with water and gentle drying at temperature lower than 80 °C.

The samples were divided into two series L and H, named from the molecular weight expected from the polymerization conditions (low and high, respectively). In both series the particle size was controlled changing the microemulsion content in the polymerization bath; moreover, in the preparation of series L the molecular weight was controlled, as well, with an appropriate use of initiator (ammonium persulfate) and transfer agent (ethane).

Sample Characterization. Particle size and shape (Table 1) were characterized using dynamic light scattering (BI9000SM, Brookhaven Instruments Co.), atomic force microscopy (Autoprobe CP, Park Scientific Instrument), and scanning (Leica Stereoscan 440) and transmission (Carl Zeiss EM900) electron microscopy.

The melt viscosity (Table 1) was measured using two different approaches, as required by the very high viscosity of some samples. For all the L samples and H1 to H4 samples, shear dynamic viscosity was measured using a Rheometric RMS 800 in the linear viscoelastic regime at 360 °C; the zero-shear rate viscosity was calculated from dynamic viscosity data using the Ellis algorithm, as embedded in Rheometrics Orchestrator software. The viscosity of samples H5 and H6 was obtained using a homemade constant stress rheometer from the shear creep compliance and recovery curves at 360 °C, as described in the literature;[22] the estimated shear rate of these measurements is about 10^{-8} s^{-1}.

Differential scanning calorimetry (DSC) was performed using two different instruments, a Perkin-Elmer DSC 7 (at Solvay Solexis) and a TA Instruments model 2920 (at the University of Padova), both operating under a N_2 atmosphere. The same procedure for melting and crystallization was used in both locations, and a high repeatability was obtained; in the first heating run, the samples were heated to 370 °C at 10 °C/min to determine their melting temperature and enthalpy; then the samples were cooled to 250 °C, at the same rate, to determine the crystallization temperature T_c and the relative enthalpy ΔH_c, and finally, the second melting was determined by heating under the same conditions of the first heating run. The room temperature transitions were studied heating the samples from −20 to 50 °C at 10°/min for both the virgin powders and the melt-crystallized samples (mc). In all cases, polymer samples weighing 6−9 mg closed in aluminum pans were used.

The results relative to the melting and crystallization parameters of virgin powders were obtained at Solvay Solexis (columns 1−6 of Table 2), while the other calorimetric results were obtained in Padova (columns 7 and 8 of Table 2 and Table 3).

The degree of crystallinity Φ_{DSC} was evaluated as

$$\Phi_{DSC} = \Delta H_m / \Delta H_{100}$$

where $\Delta H_{100} = 82.05$ J/g[23] is the melting enthalpy for a 100% crystalline sample of PTFE.

The wide-angle X-ray scattering (WAXS) patterns were recorded in the diffraction angular range 10°−80° 2θ by a Philips X'Pert PRO diffractometer, equipped with an Anton Paar TTK450 temperature control cell. Therefore, WAXS patterns of the samples in the different crystalline phases, and also in the molten phase, could be obtained. The PTFE virgin powder samples were analyzed at different temperatures without any further preparation. The melt-crystallized samples were analyzed at room temperature after being transformed into 3 mm thick films. The films were made by compression molding at room temperature (except for samples H5 and H6, which have been compressed at 350 °C), followed by free melting in an oven at 350 °C; finally, the samples were cooled by switching off the oven. The cooling rate in the crystallization range was about 1 °C/min.

Results and Discussion

Basic Sample Characterization. A preliminary discussion is necessary to elucidate the characteristics of the samples, with particular reference to the particle size and the molecular weight. This discussion is particularly important for the determination of molecular weight, which until recently has not been obtained for PTFE by standard methodologies, but only by indirect methods.[24] The relevant results are reported in Tables 1 and 2.

The average value of the particle radius was obtained by dynamic light scattering measuring the autocorrelation function of both the polarized (VV) and depolarized (VH) component.[25] This was possible because PTFE latexes are crystalline and the scattered light is strongly depolarized.[26,27] Therefore, both the translational (D_T) and rotational (D_R) diffusion coefficients could be measured, and the radius R of the equivalent sphere was calculated applying the Stokes−Einstein and the Perrin equation, respectively.[25]

$$D_T = \frac{k_B T}{6\pi\eta R}, \quad D_R = \frac{k_B T}{8\pi\eta R^3}$$

As only D_R could be measured on all the samples, we will use the radius obtained from the Perrin equation, in the following, to have an indication of the particle size (Table 1).[28]

The morphological aspects of the particles were first evaluated by light scattering, on the samples for which both diffusion coefficients could be measured. In fact, the same radius R is obtained from D_T and D_R only for spherical particles.[29] A difference between the radii obtained from rotational and translational diffusion coefficients larger than the experimental uncertainty of

Table 2. DSC Parameters Relative to First (Index m1) and Second (Index m2) Melting and Crystallization (Index c) for the Virgin Samples and Relative to First Melting of the Melt-Crystallized Samples (mc)

sample	ΔH_{m1} (J/g)	T_{m1} (°C)	ΔH_c (J/g)	T_c (°C)	ΔH_{m2} (J/g)	T_{m2} (°C)	ΔH_m(mc) (J/g)	T_m(mc) (°C)
L1	70.7	327.2	80.4	312.1	81.5	329.2	77.8	329.6
L2	68.6	327.2	77.8	311.4	77.9	329	73.2	329.8
L3	73.7	326.4	80.2	311.9	80.8	328.3	66.5	328.7
L4	74.3	326.5	77.6	312.2	78.5	327.8	59.9	329.8
H1	69.6	328.1	73.7	310.8	74.4	330.4	76.8	331.4
H2	76.4	330.5	62.3	310.1	63.2	330.1	69.8	332.3
H3	75.3	329.3	66.4	310.8	66.9	330.2	73.0	332.1
H4	78.2	330.6	61.0	311.1	61.0	329.7	61.4	332.6
H5	80.0	343.4	33.0	314.6	34.0	327.2	20.4	329.5
H6	78.6	346	32.2	314.2	32.2	326.8	20.7	327.5

Table 3. Transition Temperatures and Enthalpy for Solid−Solid Transitions of the Virgin Powders and of the Melt-Crystallized Samples (mc)

sample	$T_{II\to IV}$ (°C)	$T_{IV\to I}$ (°C)	ΔH_{II-I} (J/g)	$T_{II\to IV}$(mc) (°C)	$T_{IV\to I}$(mc) (°C)	ΔH_{II-I}(mc) (J/g)
L1	6.7		6.3	20.4	29.4	11.5
L2	8.5		7.2	20.2	29.2	13.3
L3	13.6		8.0	19.8	28.6	11.7
L4	14.1		9.9	20.4	29.1	11.5
H1	12.2		8.7	21.3	30.1	10.9
H2	15.8		9.1	21.4	30.0	10.6
H3	15.1		8.4	22.3	30.6	9.9
H4	18.8	28.8	11.0	22.9	30.9	7.9
H5	21.2	30.3	13.9	21.8	30.0	3.3
H6	20.9	30.2	14.3	20.6	29.6	4.3

the measurement (5−10%) was found for series H. In this case, the measurements were consistent with short rods having an axial ratio about 2−5, as already reported in the literature for similar standard PTFE latexes.[27,30]

The particle shape was evaluated more accurately by microscopy for all the samples (Figure 1).

As a general conclusion, combining the results of light scattering and microscopy, series H was mainly composed of rodlike particles with an axial ratio smaller than 5, while the low molecular weight series L contained only spherical particles. It is important to realize that, differently from what is reported in the literature for low molecular weight PTFE, no fibrillar particle morphology (long thin rod) were observed throughout the present work, as a consequence of the chosen polymerization method.[31]

The second relevant parameter is the molecular weight. Its determination for PTFE is very difficult, and usually relative methods are used. In this work we characterized the molecular weight using two of these methods, melt viscosity, and enthalpy of crystallization. The values of molecular weight, reported in Table 1, were obtained using published melt viscosity data for some PTFE samples of known molecular weight.[32] From the data reported by Chu et al., a $\eta-M$ relationship at 360 °C was calculated ($\eta = 2.3 \times 10^{-14}\bar{M}^{3.3}$) and used to convert our viscosity data. While the enthalpy of first melting is substantially independent of the molecular weight, the enthalpy of crystallization shows an inverse dependence on the average molecular weight[9] ($\bar{M}_n = 2.1 \times 10^{10}\Delta H_c^{-5.16}$), which is related to the progressively increasing difficulty of high-viscosity PTFE to crystallize.[33] For this reason, the crystallization enthalpy was used as an indirect measurement of the molecular weight. As a check of the good internal congruency of our results, the melt viscosity and enthalpy of crystallization are shown in Figure 2.

The comparison of molecular weight indexes and particle radius is separated in Figure 3. It is evident

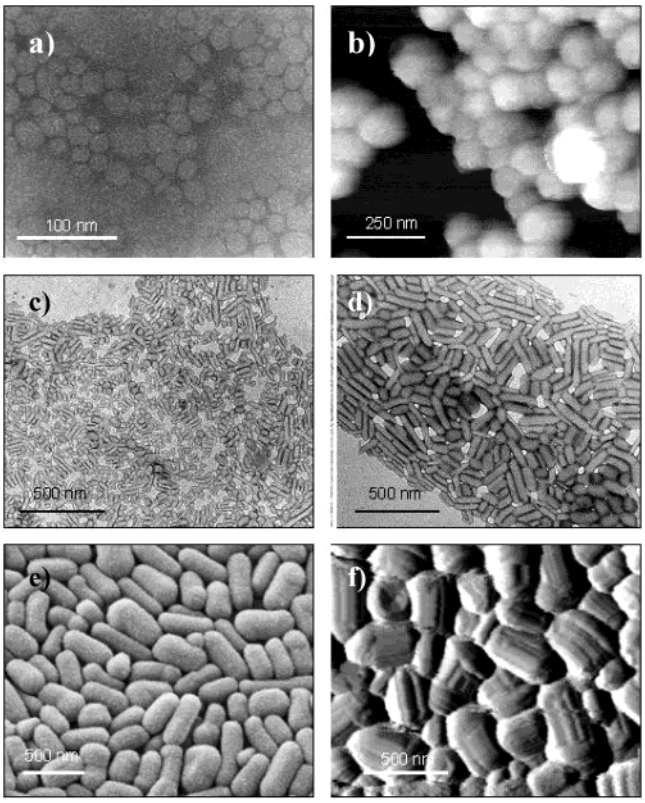

Figure 1. Microscopy pictures of the samples: (a) sample L1 (TEM), (b) sample L3 (AFM), (c) sample H2 (TEM), (d) sample H4 (TEM), (e) sample H5 (SEM), (f) sample H6 (AFM).

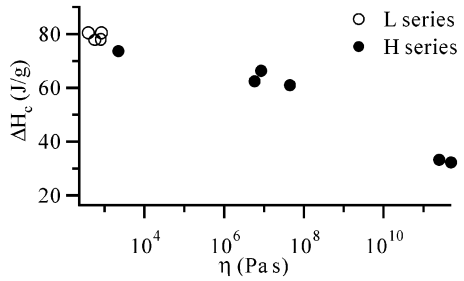

Figure 2. Crystallization enthalpy (ΔH_c) as a function of melt viscosity (η) for virgin powder samples.

that for series L molecular weight is low and independent of the particle size, while for series H it is generally higher and increases with the radius.

In Table 2 the results obtained from DSC analysis are reported for first melting, first crystallization, and second melting. Of all the studied virgin samples, just samples H5 and H6 showed a distinct second melting peak with a definitely higher melting temperature

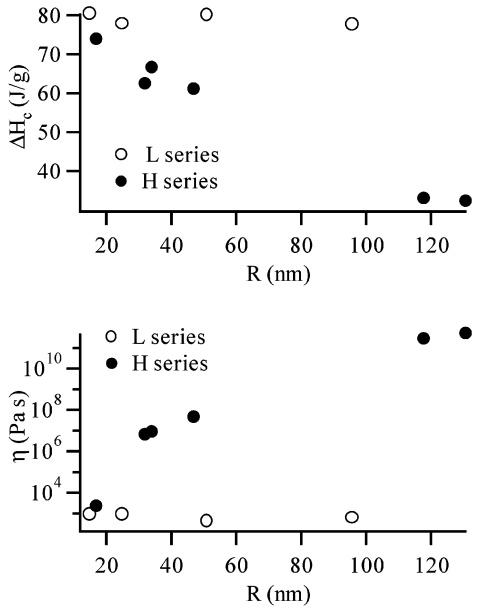

Figure 3. Crystallization enthalpy (ΔH_c) and melt viscosity (η) as functions of particle radius (R) for virgin powder samples.

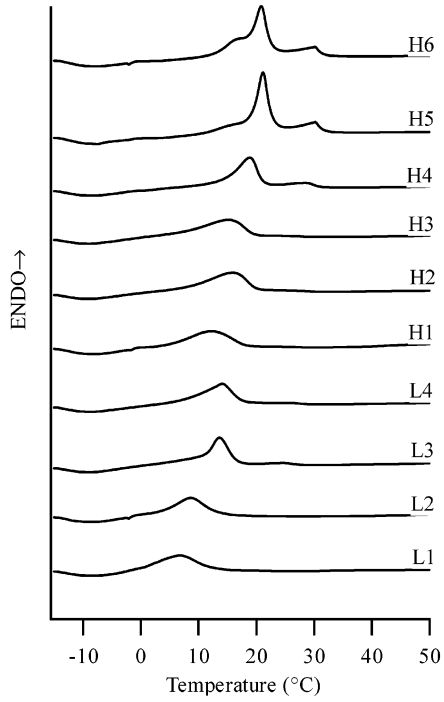

Figure 4. DSC traces relative to the solid−solid transition of the virgin powder samples.

(343−346 °C) than the rest of the samples, characterized by a melting point ranging from 326 to 330 °C. This behavior is in agreement with other studies on the dependence of melting features of virgin PTFE on the molecular weight.[9,10]

The data reported in Table 2 also show that all the samples of series L have the same first melting point independent of the particle size; therefore, the increase of T_{m1} observed from sample H1 to H6 can be attributed to the increase in molecular weight of this series. We will not discuss further these results because any trend that can be obtained from these data must be depurated from the effects of the thermal history, as virgin high molecular weight PTFE shows a strong superheating and a dependence on the heating rate, which was attributed to the presence of extended crystals which melt at high temperature.[34]

In the next two sections the main experimental findings are reported grouped according to the experimental technique, DSC and WAXS, for both virgin powders and melt-crystallized samples. The focus is on the solid−solid state transition occurring around room temperature.

Differential Scanning Calorimetry. All the samples were analyzed by DSC to determine the dependence of the temperature and the enthalpy of the solid−solid transitions, occurring in the range 0−30 °C, on the molecular weight and on the particle dimension.

Within the large amount of literature on the solid−solid transitions of PTFE,[11−18] some authors have investigated more deeply their calorimetric behavior.[34−36] In virgin PTFE homopolymer from emulsion polymerization, the DSC trace reveals the presence of three peaks which occur at about 16, 19, and 30 °C. The two peaks at high temperature are also found after recrystallization from the melt and have been associated with the transition II → IV and IV → I,[12,13] respectively. The third (lowest) peak has been reported only for emulsion polymerized PTFE[34] and was shown to be influenced by the thermal history.[35]

The presence of solid−solid transition was detected also in tetrafluoroethylene (TFE) copolymers.[36] It was shown on melt-crystallized polymers that the increase of hexafluoropropene (HFP) content induces the decrease of the transition enthalpy, the rapid disappearance of the IV → I peak, and the shift of the remaining II → IV peak toward low temperatures. This behavior was associated with the additional disorder introduced by the comonomer, which reflects in both the introduction of helix reversals and side units and the thinning of the lamellar thickness.

Figure 4 shows the DSC thermograms for all the virgin samples analyzed in the present work. Only the two highest molecular weight samples (H5, H6) show the typical DSC traces of virgin emulsion PTFE with three peaks, whose temperatures are in good agreement with the literature, while all the other samples show traces that are both qualitatively and quantitatively different.

The main differences between samples H5 and H6 and the other samples, observed decreasing the particle size and/or the molecular weight, can be summarized in (a) the decrease of the overall enthalpy associated with these transitions (Table 3), (b) the absence of the lowest temperature transition (16 °C), (c) the shift of the most intense peak (II → IV) to temperatures lower than 20 °C, and (d) the strong decrease of the DSC signal associated with the IV → I transition. (In Figure 4, this transition is clearly visible only for sample H4; however, some residual enthalpy is also present for samples L3, L4, H1, H2, and H3.)

The strong effect of molecular weight on the II → IV transition can be ascribed to the high energy required to change the crystalline symmetry from triclinic to hexagonal, which corresponds to a higher value of ΔH, in comparison with the IV → I transition, connected to a change between hexagonal and pseudohexagonal symmetry, requiring a lower energy and corresponding to a lower value of ΔH. This determines a gradual decrease of the enthalpy associated with the IV → I transition with the diminution of molecular weight because shorter chains can more easily reorganize

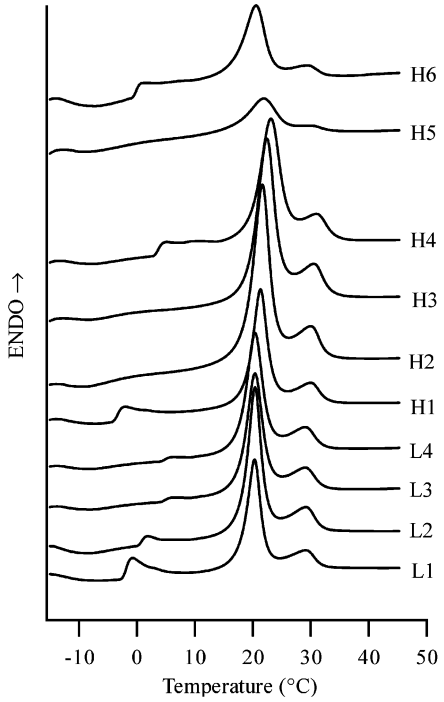

Figure 5. DSC traces relative to the solid−solid transition after crystallization from the melt.

themselves. If in fact the transition is detectable up to sample L3, in the case of L1 and L2 this is not visible because the diminution of the particle size is added to the effect of molecular weight (Table 1).

The change of the DSC pattern of the transitions with particle size/molecular weight is similar to the one found for TFE−HFP copolymers upon increasing the comonomer content.[36]

The solid−solid transitions were analyzed for the same samples after crystallization from the melt. Through this investigation we would get some helpful results to discriminate between the role of molecular weight and particle size. The characterization of their melting behavior (see the last two columns of Table 2) indicates that the enthalpy of melting decreases with the molecular weight, as expected, while the melting temperature shows a much lower dependence.

As far as it concerns the solid−solid transitions, all the melt-crystallized samples show a similar behavior, quite different from the virgin powders (Figure 5 and Table 3).

In all the DSC traces, the presence of two endothermic peaks at the same temperatures, near the values reported in the literature, is clearly evident and is independent of the sample. Moreover, in a parallel way to the amount of crystallinity (see below), the enthalpy associated with the solid−solid transitions decreases upon increasing the molecular weight. Therefore, the thermal behavior around room temperature is completely changed after crystallization from the melt. While this is an obvious finding for the particle size, as the melting is expected to destroy the memory of the particle, it is important to realize that, in the investigated samples, the molecular weight has an effect only on the amount of crystalline phase, but no effect is present on the transition temperatures as well as on the melting point. This behavior is quite different from what reported for perfluoroalkanes C_nF_{2n+1} ($n < 24$), whose melting and solid−solid transition temperatures

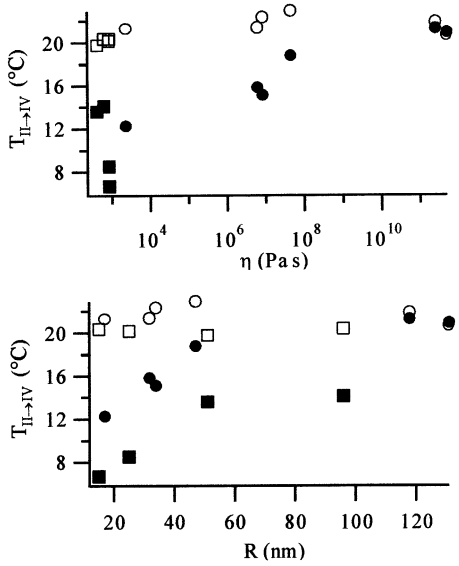

Figure 6. Phase II → IV transition temperature ($T_{II\rightarrow IV}$) as a function of melt viscosity (η) and particle size (R) for virgin powders (■, L samples; ●, H samples) and after crystallization from the melt (□, L samples; ○, H samples).

Table 4. Degree of Crystallinity Calculated by DSC for the Virgin Powder Samples (Φ) and of the Melt-Crystallized Samples (Φ_{mc})

sample	F (%)	Φ_{mc} (%)	sample	Φ (%)	Φ_{mc} (%)
L1	89.8	94.8	H2	94.4	85.1
L2	80.6	89.2	H3	95.4	89.0
L3	94.9	81.0	H4	91.8	74.8
L4	89.8	73.0	H5	99.0	24.9
H1	88.8	93.6	H6	95.4	25.2

strongly depend on the molecular weight.[37] The independence of the transition on the molecular weight can be ascribed to the much lower amount of chain ends in the present samples.

The dependence of the temperature of the II → IV transition on the melt viscosity and particle radius is illustrated in Figure 6.

For both series the virgin samples show a similar trend with an increase of $T_{II\rightarrow IV}$ up to reach a constant value, when the particle radius is higher than about 50 nm. After melting, the phase II → I transition becomes independent of both melt viscosity and particle size (see above).

The crystallinity, evaluated by the melting enthalpy ΔH_{m1} of the DSC thermogram, shows an increase with the molecular weight in the virgin powder samples (Table 4); actually, the lowest crystallinity value is 80.6% in sample L2 and the highest one is 99.0% in sample H5, but there is no evident trend with respect to different particle size, among the samples homogeneous for molecular weight.

In the samples after the compression molding, we can note (Table 4) a sensible decrease of Φ_{DSC}, especially for those with very high molecular weight. That is probably due to the difficulty of movement and of regular packing, for chains of considerable length, when the material is in the molten state; actually, in such a state, it presents a very high viscosity.

This is also confirmed by the small value of crystallization enthalpy ΔH_c (Table 2) obtained for samples H5 and H6. It is then possible to deduce that in the polymerization phase the samples with increasing molecular weight reach a higher degree of order, while such

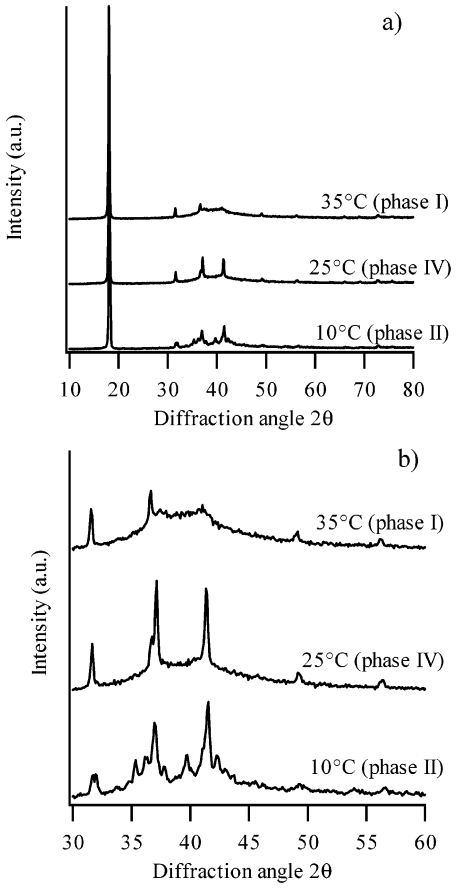

Figure 7. X-ray diffraction pattern of the virgin powder H2 sample at 10, 25, and 35 °C in the angular range 10°−80° 2θ (a) and 30°−60° 2θ (b).

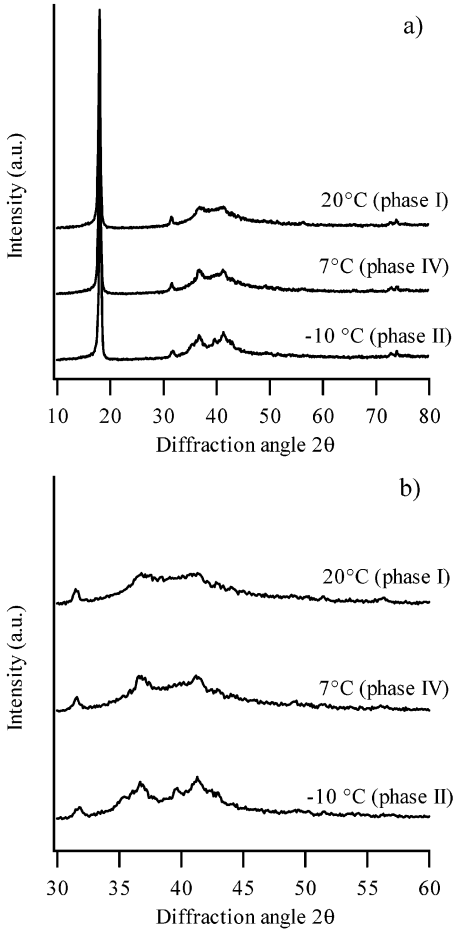

Figure 8. X-ray diffraction pattern of the virgin powder L1 sample at −10, 7, and 20 °C in the angular range 10°−80° 2θ (a) and 30°−60° 2θ (b).

a high molecular weight becomes an impediment to the ordered organization of the chains when the samples are melted, e.g., in the compression molding process.

Wide-Angle X-ray Scattering. The WAXS instrumentation available has allowed the collection of the X-ray diffraction spectra of the virgin powder samples at different temperatures. A specific temperature program was chosen for each virgin powder sample on the basis of the corresponding thermogram (Figure 4) to obtain the diffraction patterns of the different crystalline phases characteristic of the PTFE samples.

In Figures 7 and 8 the spectra collected at different temperatures for the virgin powder samples H6 (at 10, 25, and 35 °C) and L1 (at −10, 7, and 20 °C) are reported. The main reflection (2θ = 18.15°) is substantially independent of the samples and of the temperature, while the most relevant variations are those regarding the reflections between 30° and 60° 2θ.

Sample H6 (Figure 7b) shows a behavior for the solid−solid transition typical of the homopolymer like that reported in the literature, as expected from the analysis of the corresponding thermogram (Figure 4).

Below 19 °C there is the presence of phase II, phase IV appears in the range from 19 to 30 °C, and phase I forms over 30 °C.

Sample L1 (Figure 8b), on the other hand, is in the crystalline phase II at a temperature far below 19 °C: actually we registered an X-ray spectrum corresponding to the triclinic phase at −10 °C and noted the presence of phase IV at 7 °C and of phase I at 20 °C.

From the thermograms of the melt-crystallized samples (Figure 5) we can deduce that for all of them solid−solid transitions appear at temperatures near the values reported in the literature. The WAXS spectra registered at 25 °C confirm the presence, at this temperature, of phase IV for all the melt-crystallized samples.

So, it is evident the influence of the particle size on the different behavior, as regards the solid−solid transitions, of the virgin powder samples and, on the contrary, the lack of influence of the molecular weight.

It is interesting to analyze the average size of the crystallites in the virgin powder and in the mc samples as well. The indicative parameter, for the calculation of the crystallites dimension, is the full width at half-maximum (FWHM) of the diffraction peak; the average crystallites size ϵ was determined by the Scherrer formula:[38]

$$\epsilon = \frac{K\lambda}{\beta \cos \theta}$$

where $K = 0.9$, λ is the wavelength of the incident radiation, β is the fwhm, and θ is the angle corresponding to the diffraction peak.

The crystallite dimension along the *x* axis was calculated on the basis of the 100 reflex detected at about 18° 2θ; Table 5 reports the results obtained for the virgin powder and the mc samples as well.

For the virgin powder samples it is possible to observe an increase of the average crystallite dimension with particle size (Figure 9). Therefore, it appears that, independently of the molecular weight and the polymerization condition, the degree of order of the crystal-

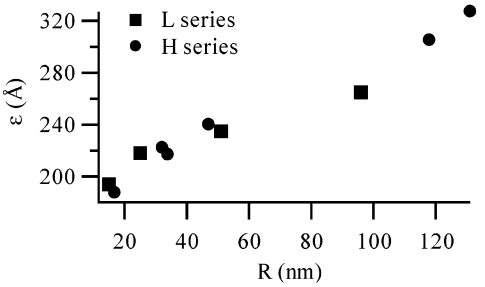

Figure 9. Average crystallite size (ϵ) as a function of particle size (R) for virgin powder samples.

Table 5. Crystallite Dimension along the *x* Axis Determined by X-ray Diffraction for the Virgin Powder Samples (ϵ) and for the Samples after Crystallization from the Melt (ϵ_{mc})

sample	ϵ (Å)	ϵ_{mc} (Å)	sample	ϵ (Å)	ϵ_{mc} (Å)
L1	194	350	H2	222	614
L2	218	438	H3	217	410
L3	235	347	H4	240	406
L4	265	314	H5	305	331
H1	188	429	H6	327	358

lites, in the virgin powders, is controlled by the particle size. In the mc samples such a behavior is not evident; however, it is possible to note that the crystallite dimension increases, in the same sample, going from the virgin powder to the mc.

Conclusions

The dependence of the crystalline structure on the particle size and the molecular weight was investigated on some PTFE virgin powders. Despite the fact that separation of the two variables is not complete, some conclusions can be drawn on their effect on the room temperature solid−solid transitions.

The polymerization of PTFE in particles having a size of few tens of nanometers depresses the thermal phenomenology of the solid−solid transition, both reducing the overall enthalpy of the transitions and shifting its temperature range toward lower values. This effect cannot be attributed to the effect of the molecular weight because after crystallizing from the melt the same polymers, in a very broad range of molecular weight, the transition assumes its typical calorimetric pattern.

The polymerization of PTFE in nanoparticles is also associated with the presence of a low degree of order, as measured by the broadening of the (100) peak, and with its increase with the particle size, independently of the molecular weight. The interpretation of the peak width as a measure of the crystal size, according to the Debye−Scherrer theory, suggests that the particle size imposes a limitation to the size of the polymer crystal formed during polymerization. This constraint is completely removed by melting.

Therefore, the confinement of the as-polymerized PTFE crystals in small entities (tens of nanometers) has a similar effect on the crystal correlation length and on the solid-state transitions, while it also appears that the molecular weight per se is not able to induce such a behavior in the melt-crystallized polymers.

The dependence of the solid−solid transition temperatures on the crystal size (Figure 10) has been already reported for a series of copolymers.[36,39] Weeks and co-workers[36] investigated the effect of comonomer on the solid−solid transition in melt-crystallized HFP−TFE copolymers. They observed the decrease upon increasing

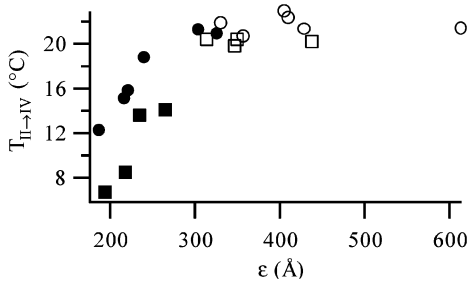

Figure 10. Phase II → IV transition temperature ($T_{II\rightarrow IV}$) as a function of the crystallite dimensions (ϵ) for virgin powders (■, L samples; ●, H samples) and after crystallization from the melt (□, L samples; ○, H samples).

the amount of comonomer, and they also correlated the decrease of solid−solid transition temperature to the decrease of the lamellar thickness, measured by small-angle X-ray scattering (SAXS).

Guerra and co-workers[39] studied the structural properties of melt-crystallized TFE copolymers with other fluorinated comonomers such as HFP, perfluoromethyl vinyl ether (MVE), and perfluopropyl vinyl ether (PVE). Among other findings, they also reported the general decrease of the Scherrer correlation length with the comonomer content. This decrease is independent of the comonomer type and parallels the decrease of the lamellar thickness independently observed on the same copolymers upon increasing the comonomer content.[40]

Acknowledgment. The support of the INSTM (Consorzio Interuniversitario Nazionale per la Scienza e Tecnologia dei Materiali) is gratefully acknowledged.

References and Notes

(1) Ebnesajjad, S. In *Non-melt Processible Fluoroplastics*; Ebnesajjad, S.; Ed.; William Andrew Publishing: New York, 2000; Vol. 1.
(2) Bladel, H.; Felix, B.; Hintzer, K.; Löhr, G.; Mitterberger, W. D. US Patent 5,576,381, 1994.
(3) Giannetti, E.; Visca, M. US Patent 4,864,006, 1987.
(4) Visca, M.; Chittofrati, A. US Patent 4,990,283, 1988.
(5) Rahl, F. J.; Evanco, M. A.; Fredericks, R. J.; Reimschuessel, A. C. *J. Polym. Sci., Part A-2: Polym. Phys.* **1972**, *10*, 1337.
(6) Smith, P.; Chanzy, H.; Revol, J.-F. *J. Polym. Sci., Polym. Lett.* **1986**, *24*, 557.
(7) Folda, T.; Hoffmann, H.; Chanzy, H.; Smith, P. *Nature (London)* **1988**, *333*, 55.
(8) Wunderlich, B. *Adv. Polym. Sci.* **1968**, *5*, 568.
(9) Suwa, T.; Seguchi, T.; Takehisa, M.; Machi, S. *J. Polym. Sci., Polym. Phys.* **1975**, *13*, 2183.
(10) Seguchi, T.; Suwa, T.; Tamura, N.; Takehisha, M. *J. Polym. Sci., Polym. Phys.* **1974**, *12*, 2567.
(11) Sperati, C. A.; Starkweather, H. W. *Adv. Polym. Sci.* **1961**, *2*, 465.
(12) Bunn, C. W.; Howells, E. R. *Nature (London)* **1954**, *174*, 549.
(13) Kilian, H. G.; Jenckel, E. *Z. Elektrochem.* **1959**, *63*, 308.
(14) Clark, E. S.; Muus, L. T. *Z. Kristallogr. Kristallgeom. Kristallphys. Kristallchem.* **1962**, *117*, 108.
(15) Clark, E. S.; Muus, L. T. *Z. Kristallogr. Kristallgeom. Kristallphys. Kristallchem.* **1962**, *117*, 119.
(16) Marega, C.; Marigo, A.; Garbuglio, C.; Fichera, A.; Martorana, A.; Zannetti, R. *Makromol. Chem.* **1989**, *190*, 1425.
(17) Flack, H. D. *J. Polym. Sci., Part A-2: Polym. Phys.* **1972**, *10*, 1799.
(18) Matsushige, K.; Enoshita, R.; Ide, T.; Yamauchi, N.; Taki, S.; Takemura, T. *Jpn. J. Appl. Phys.* **1977**, *16*, 681.
(19) Basset, D. C.; Davit, R. *Polymer* **1974**, *15*, 721.
(20) Kapeliouchko, V.; Marchese, E.; Colaianna, P. Eur. Patent 969,027, 2000.
(21) Giannetti, E.; Chittofrati, A.; Sanguineti, A. *Chim. Ind.* **1997**, *79*, 611.
(22) Ajroldi, G.; Garbuglio, C.; Ragazzini, M. *J. Appl. Polym. Sci.* **1970**, *14*, 79.

(23) Laus, F.; Suzuki, H.; Wunderlich, B. *J. Polym. Sci., Polym. Phys.* **1984**, *22*, 379.
(24) Chu, B.; Wu, C.; Buck, W. *Macromolecules* **1989**, *22*, 831.
(25) Berne, B. J.; Pecora, R. *Dynamic Light Scattering*; J. Wiley & Sons: New York, 1976.
(26) Degiorgio, V.; Piazza, R.; Bellini, T.; Visca, M. *Adv. Colloid Interface Sci.* **1994**, *48*, 61.
(27) Russo, P. S.; Saunders, M. J.; DeLong, M.; Kuehl, S.; Langley, K. H.; Detenbeck, R. W. *Anal. Chim. Acta* **1986**, *189*, 69.
(28) In fact, the depolarized component can be as high as 30% of the other component for the smallest latexes; therefore, the standard determination of the particle size from translational diffusion could not be achieved on the whole set of latexes, as it is impossible to separate the polarized and depolarized scattered light in VV geometry. A complete presentation of the light scattering characterization is outside the scope of this work, and it will be the subject of a different publication; some results were presented: Perego, A.; Sanguineti, A. *Light Scattering Study of PTFE Latexes: Effect of Particle Size and of Surfactant Adsorption*, ModPol 2003, Bratislava (SK), 5−8 Oct 2003.
(29) Chu, B. *Laser Light Scattering*; Academic Press: New York, 1974.
(30) Piazza, R.; Stavans, J.; Bellini, T.; Degiorgio, V. *Opt. Commun.* **1989**, *73*, 263.
(31) As a word of caution, we note that the quantitative comparison between the two series cannot be pushed too far as the different shape between the two series do not allow a proper comparison using the particle radius.
(32) Chu, B.; Linliu, K. *Macromolecules* **1995**, *28*, 2723.
(33) Suwa, T.; Takehisa, M.; Machi, S. *J. Appl. Polym. Sci.* **1973**, *17*, 3253.
(34) Starkweather, H. W. *J. Polym. Sci., Polym. Phys.* **1985**, *23*, 1177.
(35) Villani, V.; Pucciariello, R.; Ajroldi, G. *J. Polym. Sci., Polym. Phys.* **1991**, *29*, 1255.
(36) Weeks, J. J.; Sanchez, I. C.; Eby, R. K.; Poser, C. I. *Polymer* **1980**, *21*, 325.
(37) Starkweather, H. W. *Macromolecules* **1986**, *19*, 1131.
(38) Klug, H. P.; Alexander, L. E. *X-Ray Diffraction Procedures*; John Wiley & Sons: New York, 1974.
(39) Guerra, G.; Venditto, V.; Natale, C.; Rizzo, P.; De Rosa, C. *Polymer* **1998**, *39*, 3205.
(40) Marigo, A.; Marega, C.; Zannetti, R.; Ajroldi, G. *Macromolecules* **1997**, *29*, 2197.

MA049238O